In-situ immune profile of polymorphic vs. macular Indian Post Kala-azar dermal leishmaniasis

Ritika Sengupta[a], Shibabrata Mukherjee[a], Srija Moulik[a], Sneha Mitra[a], Surya Jyati Chaudhuri[b], Nilay Kanti Das[c], Uttara Chatterjee[d,**], Mitali Chatterjee[a,*]

[a] *Dept. of Pharmacology, Institute of Post Graduate Medical Education and Research, Kolkata, 700020, India*
[b] *Dept. of Microbiology, Govt. Medical College, Purulia, India*
[c] *Dept. of Dermatology, Bankura Sammilani Medical College, Bankura, 722102, India*
[d] *Dept. of Pathology, Institute of Post Graduate Medical Education and Research, Kolkata, 700020, India*

ARTICLE INFO

ABSTRACT

Post Kala-azar Dermal Leishmaniasis (PKDL), a sequel of apparently cured Visceral Leishmaniasis presents in South Asia with papulonodular (polymorphic) or hypomelanotic lesions (macular). Till date, the polymorphic variant was considered predominant, constituting 85–90%. However, following active-case surveillance, the proportion of macular PKDL has increased substantially to nearly 50%, necessitating an in-depth analysis of this variant. Accordingly, this study aimed to delineate the cellular infiltrate in macular vis-à-vis polymorphic PKDL. To study the overall histopathology, hematoxylin and eosin staining was performed on lesional sections and phenotyping by immunohistochemistry done in terms of dendritic cells (CD1a), macrophages (CD68), HLA-DR, T-cells (CD8, CD4), B-cells (CD20) and Ki67 along with assessment of the status of circulating homing markers CCL2, CCL7 and CXCL13. In polymorphic cases (n = 20), the cellular infiltration was substantial, whereas in macular lesions (n = 20) it was mild and patchy with relative sparing of the reticular dermis. Although parasite DNA was identified in both variants by ITS-1 PCR, the parasite load was significantly higher in the polymorphic variant and Leishman-Donovan bodies were notably minimally present in macular cases. Both variants demonstrated a decrease in CD1a$^+$ dendritic cells, HLA-DR expression and CD4$^+$ T-cells. In macular cases, the proportion of CD68$^+$ macrophages, CD8$^+$ T-cells and CD20$^+$ B-cells was 4.6 fold, 17.0 fold and 1.6 fold lower than polymorphic cases. The absence of Ki67 positivity and increased levels of chemoattractants suggested dermal homing of these cellular subsets. Taken together, as compared to the polymorphic variant, patients with macular PKDL demonstrated a lower parasite load along with a lesser degree of cellular infiltration, suggesting differences in host-pathogen interactions, which in turn can impact on their disease transmitting potential and responses to chemotherapy.

1. Introduction

The dermal variants of leishmaniasis present either as single ulcerated lesion i.e. localized self-healing cutaneous leishmaniasis (LCL) caused by *Leishmania braziliensis, L. amazonensis* and *L. mexicana,* or as lesions that are disseminated multiple ulcers and papules involving the oronasal mucosa, termed as mucocutaneous leishmaniasis (MCL), causative species being *L. braziliensis* and *L. panamensis* or in a generalised, diffuse pattern termed as diffuse cutaneous leishmaniasis (DCL), species involved being *L. mexicana* and *L. amazonensis* (Reithinger et al., 2007). In the Old world, CL is generally self-healing and is caused by *L. major, L. tropica* and *L. aethiopica* (Masmoudi et al., 2013). An interesting

dermal variant caused by *L. donovani* occurs in Sri Lanka and appears as small erythematous papules which can also assume a nodulo-ulcerative appearance (Karunaweera et al., 2003). Additionally, in North-Western India, nodulo-ulcerative lesions with crusted plaques caused by *L. tropica* have been reported (Aara et al., 2013).

To add further complexity to dermal leishmaniasis is Post Kala-azar Dermal Leishmaniasis (PKDL), which appears as a dermal sequel in patients with apparently cured Visceral Leishmaniasis (VL), the causative organism being *L. donovani.* In terms of its etiopathogenesis, it is possibly the most challenging variant of Leishmaniasis (Ganguly et al., 2010a; Zijlstra et al., 2017). As patients with PKDL harbour parasites in their dermal lesions that are easily accessible to sand flies, they act as

disease reservoirs and play a major role in the transmission cycle (Mondal et al., 2018; Molina et al., 2017). With a view to eliminating VL, from South Asia, the governments of Bangladesh, India and Nepal convened to establish a Regional Kala-azar Elimination Programme (KAEP), presently targeted for 2020 (Zijlstra et al., 2017). An important component of the KAEP is active surveillance so as to identify potential disease reservoirs, the key contributors being asymptomatic cases of VL and patients with PKDL.

Although PKDL is confined to South Asia and East Africa (mainly Sudan), they have several differences in that in South Asia, approximately 5–10% of apparently cured VL patients develop PKDL, whereas in Sudan it is 50–60%, and often concomitant with VL (Burza et al., 2018; Ramesh et al., 2015; Zijlstra et al., 2000, 2003). Furthermore, in Africa it appears as papular, macular, maculopapular, nodular or plaque-like lesions, and mostly heal spontaneously within 6 months to 1 year of their appearance (Ismail et al., 2006a). In contrast, in South Asia, PKDL is not self-healing and presents in two distinct clinical forms, i.e. a combination of macules, papules and/or nodules, referred to as 'polymorphic PKDL' or as hypopigmented patches referred to as 'macular PKDL' (Ramesh et al., 2015), and the former was earlier considered to represent over 90% of PKDL cases (Mukhopadhyay et al., 2015; Ramesh et al., 2015; Ganguly et al., 2010a). With implementation of active case surveillance in West Bengal, a huge number of macular cases were unearthed, that translated into the conventional ratio of polymorphic: macular becoming almost 1:1, i.e. macular PKDL now constitute nearly 50% of the PKDL population burden (Sengupta et al., 2019). Unlike polymorphic PKDL, macular cases pose a diagnostic dilemma as owing to the minimal presence of detectable parasites, diagnosis is solely by clinical features, and their hypopigmented lesions are often indistinguishable from other hypopigmentary disorders like vitiligo, pitryasis versicolor or leprosy (Sengupta et al., 2019). Furthermore, the hypopigmentation persists even after elimination of parasites, and therefore quantification of parasite load becomes a critical objective parameter of efficacy. In recent studies, the macular variant was less responsive to Liposomal Amphotericin B (Moulik et al., 2018), suggesting possible differences in host-parasite interactions, emphasizing the need for considering treatment stratification.

An ongoing debate regarding the role of macular cases in disease transmission was resolved by Molina et al. (2017) who in a proof-of-concept experiment established that both maculopapular and nodular PKDL lesions played a definitive role in transmission, thus countering the conventional belief that macular and papular forms pose a lesser threat than nodular PKDL. Furthermore, as both nodular and macular variants were demonstrated to be infectious to sand flies, it was recommended that treatment be accorded regardless of lesion type or disease duration (Mondal et al., 2018). In Indian PKDL, the cellular immune responses till date have always been analysed as a single entity and differences if any, between macular and polymorphic forms of PKDL remain poorly explored. The two forms differed in their proportion of activated CD4 and CD8 T-cells in the circulation (Kaushal et al., 2016), but their status at the lesional sites are yet to be defined. Similarly, histopathological studies comparing the two forms of PKDL has been conducted (Singh et al., 2015), but data comparing the immunopathology of polymorphic vs. macular variants is yet to emerge. Therefore, the immune pathways that underpin the pathogenesis of PKDL continue to remain a subject of considerable debate, with data on the macular component being fragmentary in nature. Accordingly, this study aimed to delineate and compare the *in-situ* immune profile of the two variants of PKDL in terms of their overall histopathology, especially with regard to distribution and characterization of the cellular infiltrate. Furthermore, the proliferation status of cells in the lesions were assessed in terms of Ki67 along with chemokines responsible for homing of macrophages (CCL2/7) and B-cells (CXCL13).

2. Materials and methods

2.1. Reagents

Reagents were from Sigma Aldrich (St. Louis, Mo, USA) except anti-human CD4 (clone 4B12), CD8 (clone C6/144B), CD1a (clone 010), CD68 (clone PG-M1), HLA-DR (clone TAL.1B5), CD20 (clone L26), Ki67 (clone MIB-1), secondary detection system EnVision™ G|2 System/AP-Rabbit/Mouse (Permanent Red), EnVision™ FLEX Mini Kit, High pH (DAB + chromogen), EnVision™ FLEX Target Retrieval Solution (Dako, Glostrup, Denmark), QIAmp DNA Mini kit (Qiagen, Hilden, Germany), SYBR Green qPCR Master Mix (Applied Biosystems, Grand Island, NY, USA) and Bio-Plex Pro™ Human Chemokine Panel 40-Plex (BioRad, Hercules, CA, USA).

2.2. Study population

Patients clinically diagnosed with PKDL (n = 40) were recruited from the Dermatology outpatient departments of School of Tropical Medicine/Calcutta Medical College/Institute of PG Medical Education & Research, Kolkata (2007-date) or following active field surveys conducted in Malda, Dinajpur and Birbhum districts of West Bengal by active surveillance (2014-date, Sengupta et al., 2019). The initial diagnosis was based on clinical features, a prior history of VL, rK-39 positivity, or if they resided in an area endemic for VL; subsequently, diagnosis was confirmed by ITS-1 PCR and/or Giemsa staining done on a lesional biopsy (Das et al., 2011). Healthy volunteers (n = 10) were recruited from non-endemic and endemic areas and were negative for anti-leishmanial antibodies as tested by ELISA. A dermal biopsy (4 mm) was obtained using a punch biopsy from any lesional site.

2.3. Histopathology

Formalin fixed paraffin embedded (FFPE) tissues were sectioned (3 μm), placed on poly L-lysine coated slides and examined by Hematoxylin and Eosin (H&E) for overall histopathology and Giemsa stained for detection of Leishman Donovan (LD) bodies. The cellular infiltrate was scored semi-quantitatively as 1 = mild, 2 = moderate, 3 = severe and 4 = very severe [1 = 0–25 cells/mm^2; 2 = 26–50 cells/mm^2; 3 = 51–75 cells/mm^2; 4 = > 75 cells/mm^2] (Mukherjee et al., 2015). A scoring was developed for LD bodies, wherein 1–10 parasites/1000 fields = 1+, 1–10 amastigotes/100 fields = 2+, 1–10 amastigotes/10 fields = 3+, 1–10 amastigotes/field = 4+, 10–100 amastigotes/field = 5 + and > 100 amastigotes/field = 6+. Five fields were manually counted under a light microscope (EVOS FL Cell Imaging System, Waltham, MA, USA) at 1000X magnification and the average was taken.

2.4. Immunohistochemistry

FFPE sections were deparaffinised in xylene and rehydrated using descending grades of alcohol (100-70%) and distilled water. After heat induced epitope retrieval at pH 6 or pH 9, the slides were incubated with appropriate dilutions of primary antibody (1:100 for CD1a, 1:50 for CD68, CD8, CD20, 1:40 for HLA-DR, CD4, 1:25 for Ki67) for 1 h, washed with Tris-buffered saline containing 0.05% Tween-20 (0.02M, pH 7.4, TBS-T) and incubated with EnVision™ G|2 System/AP-Rabbit/Mouse (Permanent Red) or EnVision™ FLEX Mini Kit, High pH (DAB + chromogen) as per the manufacturer's protocol and counter stained with hematoxylin. Sections from human lymph nodes, gut and skin from healthy individuals served as positive controls (Mukherjee et al., 2015). For healthy controls, 4 mm skin biopsies were obtained from laboratory volunteers (n = 4) or foreskin of males undergoing voluntary circumcision (n = 6). Five fields were manually counted

under a light microscope at 400X magnification, the average taken and expressed as cells mm^{-2}. To minimize bias, two blinded investigators independently evaluated the slides.

2.5. Quantification of circulatory CCL2, CCL7 and CXCL13

Plasma levels of CCL2, CCL7 and CXCL13 were measured (diluted 1:4), using a multiplex detection kit (BioRad, Hercules, CA, USA) as per the manufacturer's protocol. Data was acquired in a Luminex 200 Labmap system (Luminex, Austin, TX, USA) and analysed using Bio-Plex Manager software version 6.2.

2.6. Measurement of parasite load by real time PCR (rtPCR)

For measurement of parasite load, a standard curve was generated by adding a defined number of *Leishmania* parasites sourced from a *L. donovani* strain (ranging from 10 to 1×10^5) to blood (180 μl) sourced from a healthy control. Real-time PCR was performed using specific primers for minicircle kDNA (116bp, forward 5′-CCTATTTTA CACCAACCCCCAGT-3'and reverse 5′-GGGTAGGGGCGTTCTGCG AAA-3′). Briefly, DNA extraction was performed according to the manufacturer's instructions from a skin biopsy collected in phosphate-buffered saline (20 mM, pH 7.4), excised into small pieces, and DNA eluted in 50 μL of DNA elution buffer. DNA (1 μl) was then added to a 19 μl reaction mixture containing SYBR Green Master mix and 400 nM of each primer. Two negative controls were used i.e. DNA from a healthy donor (no amplification), and a reaction mixture with water instead of the template DNA (no template). The number of parasites was extrapolated from the standard curve and final parasite load determined as the number of parasites/μg genomic DNA. Parasite load < 10 (C_T value being equivalent to NTC) was given an arbitrary value of 1 (Moulik et al., 2018).

2.7. Ethics statement

The study received approval from the Institutional Ethics Committee of School of Tropical Medicine, Kolkata and Institute of Post Graduate Medical Education and Research, Kolkata and all experiments were performed in accordance with relevant guidelines and regulations. Individuals or their legally acceptable representative (if < 18 years) gave a written informed consent. Informed consent was also obtained to publish after maintaining patient confidentiality information/images in an online open-access publication.

2.8. Statistical analysis

Results were expressed as median (Interquartile range, IQR) and data analysed between groups by Kruskal wallis test followed by Dunn's multiple comparison test for non-parametric data, while paired data were analysed using Student's t-test (for parametric data). Correlation was by Pearsons correlation for parametric data and Spearman's rank correlation for nonparametric data using GraphPad Prism software (version 5.0, GraphPad software Inc., La Jolla, CA, USA), p < 0.05 being significant.

3. Results

Active surveillance for PKDL unearthed a substantial proportion of macular PKDL and altered the conventional demographic scenario of PKDL, with the ratio of polymorphic:macular PKDL changing from 9:1 (Mukhopadhyay et al., 2015; Ramesh et al., 2015) to almost 1:1 (Sengupta et al., 2019). Accordingly, the study population included patients with polymorphic (n = 20) and macular PKDL (n = 20). Amongst the polymorphic cases, 7 were obtained following passive surveillance and 13 following active surveillance, whereas all 20 macular cases were by active case detection. The median age, in years, was

Table 1
Study population.

Characteristics	Patients with PKDL		Healthy controls (n = 10)
	Polymorphic (n = 20)	Macular (n = 20)	
Age (years)[a]	25.50(19.00–38.75)	17.50(10.00–33.00)	4(2.75–26.25)
Sex ratio (M:F)	2.3:1	1:1.5	4:1
Disease duration (years)[a]	0.83(0.42–4.00)	0.75(0.30–2.00)	NA
Interval between VL and PKDL (years)[a]	5.00(3.00–7.00)	3.00(2.00–4.00)	NA

M = Male; F = Female; NA = Not applicable; PKDL = Post Kala-azar Dermal Leishmaniasis; VL = Visceral Leishmaniasis.
[a] Values are expressed as median (IQR).

comparable between the two groups (Table 1), but in the polymorphic variant, there was a male preponderance which was absent in the macular cases (Table 1). Only one patient did not give a prior history of VL (Table 1). Regarding their treatment for VL, the polymorphic cases received Sodium antimony gluconate (SAG, 18/19) and one received Miltefosine. However, in the macular group, treatment was with SAG (n = 11), Miltefosine (n = 7) or Liposomal Amphotericin B (LAmB, n = 2).

In terms of distribution of lesions, there were lesions distributed asymmetrically in the polymorphic cases and predominantly on the sun exposed areas e.g. chin, nose, ears, lips and neck and occasionally on the limbs (Fig. 1a), and the number of lesions ranged from 10 to 12 (Fig. 1a). However, in the macular variant, lesions were generally symmetrically distributed (Fig. 1b), and diffusely scattered all over the body (head, neck, trunk, upper and lower limbs), Fig. 1b.

All patients were ITS-1 PCR positive and quantification of the parasite load by qPCR, showed that the median parasite number was 20.8 fold higher in the polymorphic group being 177348(11966-380513) vs. 8506(3572–67166)/μg genomic DNA, p < 0.05, Fig. 1c. In polymorphic lesions, Leishman-Donovan (LD) bodies were identified (Fig. 1d), whereas no LD bodies were detected in macular cases, even when the parasite load was high. In majority of the polymorphic cases (14/20, 70%), LD body score was 5 + while in the rest, score was 4 +. In polymorphic PKDL, the number of LD bodies correlated positively with the cell infiltration (cells/mm²), r = 0.44.

3.1. Distribution of cellular infiltrate

In both variants, there was a diffuse inflammatory cellular infiltrate which was primarily in the dermis in polymorphic cases, whereas in the macular variant, it was patchy, perivascular and periappendageal (Fig. 2a). The infiltrate in both variants comprised of lymphocytes, macrophages and plasma cells in the ratio of 4:5:1. In 70% of the polymorphic cases, the infiltrate occupied almost the entire dermis, whereas in the macular variant, it was present usually as clusters in the papillary dermis (Fig. 2a). The density of the cellular infiltrate in polymorphic PKDL ranged from moderate to severe, whereas in macular PKDL it was mild or sparse, median(IQR) being 2(1–3) vs. 1(1-1), Fig. 2b. In both types, the extent of the cellular infiltrate (cells/mm²) strongly correlated with the parasite load, being r = 0.54, p < 0.05 in the polymorphic cases (Fig. 2c) and r = 0.73, p < 0.001 (Fig. 2d) in the macular cases. With treatment, both variants demonstrated a pronounced decrease in the cell infiltrate (Fig. 2a). A narrow band of clear, sub-epidermal Grenz zone was evident in 13/20 polymorphic cases, but was limited to only 7/20 in the macular group (Fig. 2e). In both the clinical variants of PKDL, there was absence of epitheloid granulomas with giant cells (Fig. 2a). Also, unlike leprosy, the neural Schwann cells were unaffected and did not harbour parasites; furthermore, these patients reported no loss of sensation.
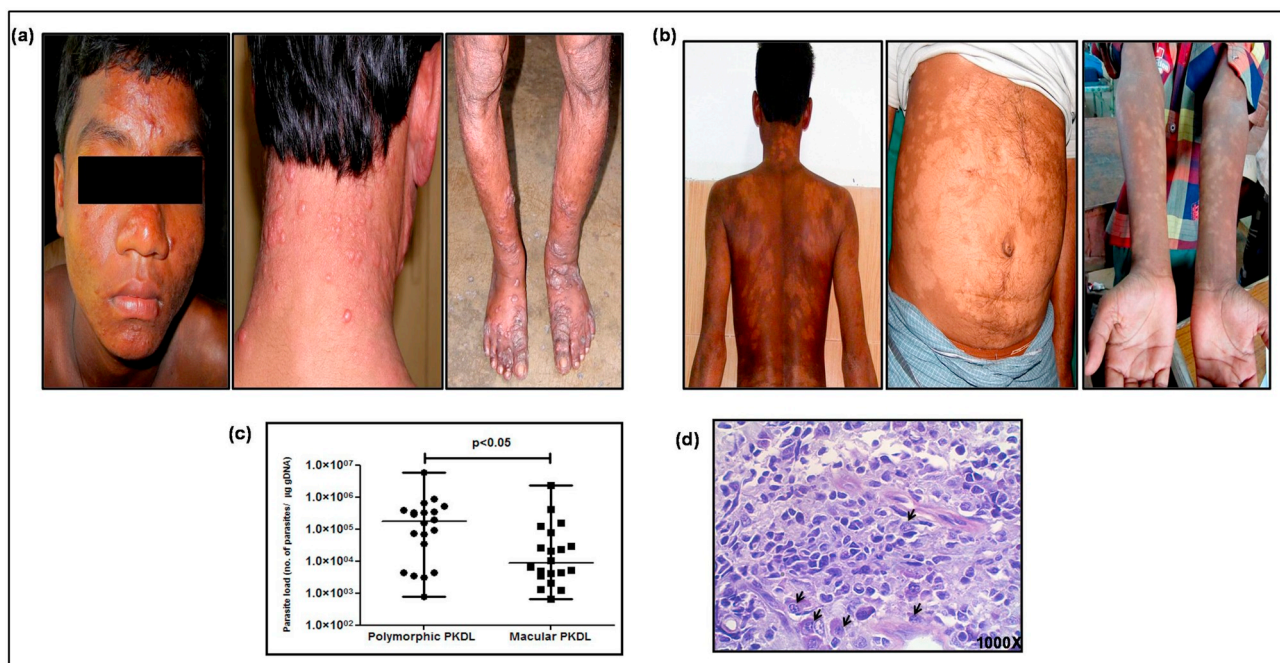
Fig. 1. a. Representative profiles of patients with polymorphic PKDL showing distribution of lesions.

b. Representative profiles of patients with macular PKDL showing distribution of lesions

c. Scatter plots showing parasite load (number of parasites/µg of genomic DNA) in patients with polymorphic (filled circle, n = 20) and macular (filled square, n = 20) PKDL. Each horizontal bar represents the median value.

d. Representative profile of a Giemsa stained dermal section of a patient with polymorphic PKDL showing amastigotes (indicated by black arrows, 1000X magnification).

3.2. Epidermal changes

In polymorphic and macular PKDL, lesions in the epidermis demonstrated hyperkeratosis, focal papillomatosis, epidermal thinning and follicular plugging (Fig. 2e, Table 2) in varying degrees; hyperkeratosis was more frequently present in the polymorphic vs. macular cases [14/20 vs. 8/20, 31.41(22.62–58.72)µm vs. 21.95(14.37–30.81)µm, p < 0.05, Fig. 2e]. Similarly, papillomatosis and elongation of rete ridges was more frequently evident in polymorphic (15/20, 75%) *vis-a-vis* macular cases (8/20, 40%), Fig. 2e, Table 2. In terms of epidermal thickness, it was significantly decreased in polymorphic cases as compared to healthy controls, 62.21(56.71–67.41) vs. 91.60(68.49–120.10) µm, p < 0.01; the scenario was similar in macular cases [52.37(39.98–60.78) µm, p < 0.001], Fig. 2e. Treatment translated into epidermal thickening, both in polymorphic [102.90(43.04–157.4) µm] as well as macular PKDL [80.6(39.98–60.78) µm]. However, hyperkeratosis persisted in 60% of the polymorphic and 70% of the macular cases (Fig. 2a).

3.3. Absence of proliferation at the dermal site in polymorphic and macular PKDL

The expression of Ki-67 protein is associated with cell proliferation and is present during all active phases of the cell cycle (Scholzen and Gerdes, 2000). Both polymorphic and macular PKDL did not demonstrate any positive staining for Ki67, thus indicating that the cells at the dermal lesions are non-proliferative in nature and have been homed to the lesional sites (Fig. 2f).

3.4. Langerhans cells decreased in polymorphic and macular PKDL

Dendritic cells (DCs) are the major immune sentinels in the skin and are present as epidermal Langerhans cells (LC) and dermal DC (dDC), both identifiable by staining with CD1a (Mukherjee et al., 2015). In

both variants, there was a loss of characteristic spindle shaped cells with dendritic processes, and instead cells had a more circular pattern (Fig. 3a). At disease presentation, polymorphic PKDL demonstrated a significant 3.07 fold decrease in LCs as compared to healthy controls [6.00(3–10.65) vs. 18.40(17.75–20.60) cells mm^{-2}, p < 0.001]; similarly, the macular cases showed a significant 1.74 fold decrease [10.60(9.10–11.50) cells mm^{-2}, p < 0.05], Fig. 3b.

With regard to dermal DCs, as compared to healthy controls there was a substantial 9.06 fold decrease in the polymorphic variant [1.70(0.75–3.00) vs. 15.40(13.85–17.90) cells mm^{-2}, p < 0.01] and a 3.85 fold decrease in macular cases [4.00(0.50–7.10) cells mm^{-2}, p < 0.01] (Fig. 3a and b). However, irrespective of the variant, the dendritic cells poorly correlated with parasite load (r = 0.03 and 0.01) with regard to polymorphic and macular PKDL respectively.

3.5. Decrease in HLA-DR was greater in macular PKDL

Antigen presenting cells use HLA-DR, a major MHC (major histocompatibility complex) class II cell surface receptor to present processed antigenic peptides for recognition by T-cells. In polymorphic PKDL, the HLA-DR expression was lower than healthy controls [8.20(6.80–10.30) vs. 13.80(7.00–18.20) cells mm^{-2}], whereas in the macular group, it was significantly lowered by 4.3 fold as compared to controls [3.20(1.35–5.55) cells mm^{-2}, p < 0.01], Fig. 3c and d. In both variants, the correlation between HLA-DR$^+$ cells and parasite load was weak, being r = 0.17 and 0.03 with regard to polymorphic and macular PKDL respectively.

3.6. Increased presence of CD68$^+$ macrophages limited to polymorphic PKDL

Pathogens including *Leishmania* must evolve ways to circumvent the antimicrobial strategies adopted by macrophages (Arango Duque and Descoteaux, 2015). In Indian PKDL, an increased presence of
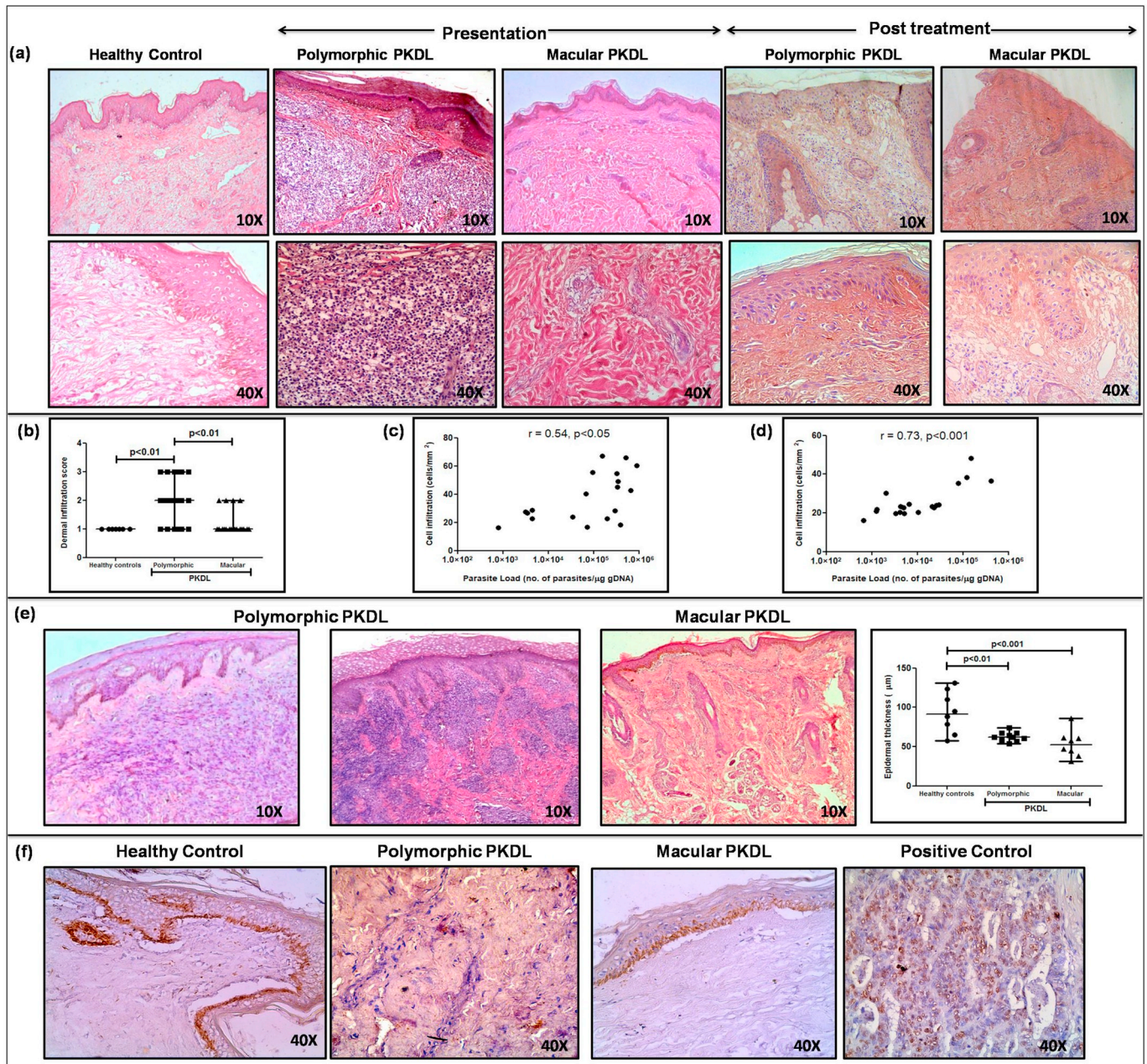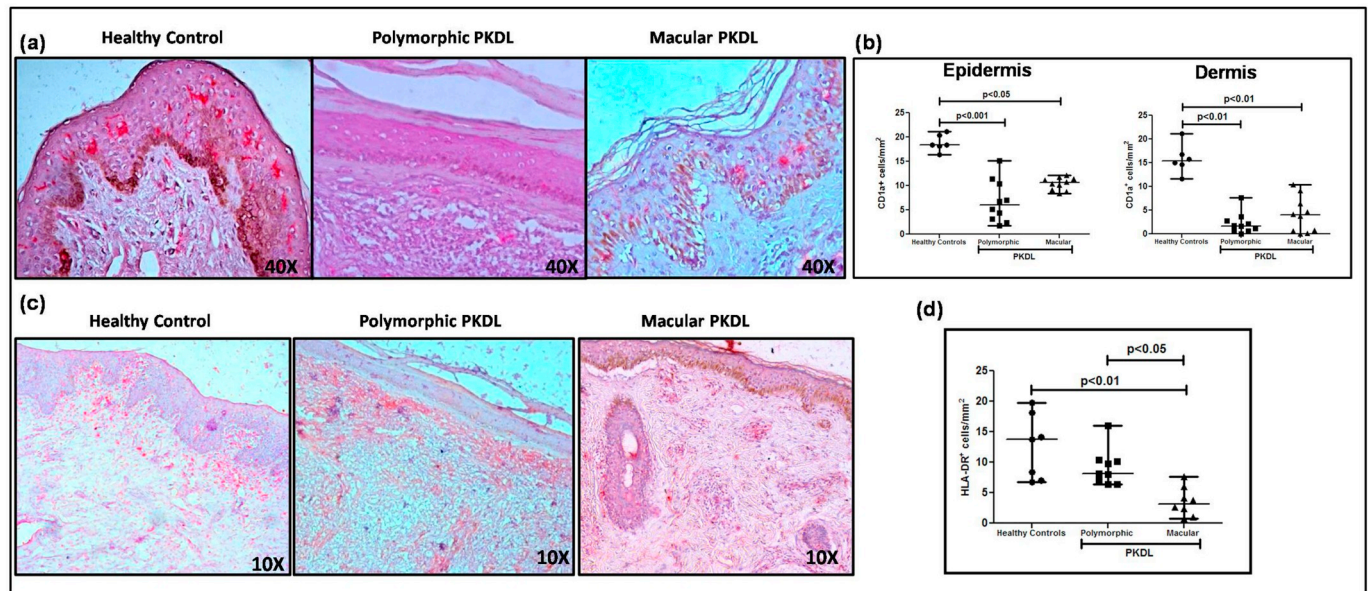
Fig. 2. a. Representative profiles of H&E stained sections from dermal biopsies of a healthy control, patient with polymorphic and macular PKDL at disease presentation and post treatment (10X and 40X magnification).

b. Scatter plots showing the dermal infiltration score of healthy controls (filled circle, n = 7), patients with polymorphic (filled square, n = 20) and macular (filled triangle, n = 20) PKDL. Each horizontal bar represents the median value.

c. Correlation of parasite load (no. of parasites/μg genomic DNA) in patients with polymorphic PKDL with their cellular infiltration (cells/mm^2).

d. Correlation of parasite load (no. of parasites/μg genomic DNA) in patients with macular PKDL with their cellular infiltration (cells/mm^2).

e. Representative histological profile from a dermal biopsy of a patient with polymorphic PKDL showing epidermal thinning, presence of a clear Grenz zone, hyperkeratosis and papillomatosis (10X magnification). Representative histological profile from a dermal biopsy of a patient with macular PKDL showing epidermal thinning and follicular plugging (10X magnification). Scatter plots of epidermal thickness (μm) in healthy controls (filled circle, n = 8), patients with polymorphic (filled square, n = 10) and macular (filled triangle, n = 8) PKDL. Each horizontal bar represents the median value.

f. Representative IHC profiles of Ki67 from dermal biopsies of a healthy control, patient with polymorphic and macular PKDL; gut mucosal tissue served as a positive control (40X magnification).

alternatively activated macrophages at lesional sites has been demonstrated (Mukhopadhyay et al., 2015), but the study focused on the polymorphic variant. At disease presentation, there was an increased infiltration of CD68$^+$ cells in polymorphic and macular PKDL, being 10.75 fold higher in polymorphic PKDL as compared to healthy controls, 60.2(15.5–99.8) vs. 5.6(2.5–10.4) cells mm^{-2}, p < 0.05 and only 2.3 fold in macular PKDL [13.1(2.25–19.05) cells mm^{-2}, Fig. 4a

and b]. The parasite load correlated positively with CD68$^+$ cells in polymorphic PKDL (r = 0.59), whereas in macular PKDL it correlated negatively (r = −0.41). In terms of disease duration, CD68$^+$ cells showed a negative correlation in polymorphic (r = −0.41) and macular (r = −0.47) PKDL. The levels of chemokines, CCL2 (MCP-1) and CCL7, responsible for the dermal homing of macrophages were raised by 3.7 and 1.7 fold respectively as compared to healthy controls being

Table 2

Histopathological changes in polymorphic and macular PKDL.

Features	Polymorphic PKDL	Macular PKDL
Hyperkeratosis	More frequent (14/20)	Less frequent (8/20)
Papillomatosis	More frequent (15/20)	Less frequent (8/20)
Epidermal Atrophy	Present	Present
Follicular Plugging	Present	Present
Sub-epidermal clear Grenz zone	More frequent (13/20)	Less frequent (7/20)
Intensity of dermal cell infiltrate	Moderate to severe	Mild to moderate
Distribution of cell infiltrate	Diffuse, occupying the entire dermis	Patchy perivascular and periappendageal, mainly in the papillary dermis
Leishman-Donovan (LD) bodies	Present	Absent
Composition of the cell infiltrate	Majority macrophages and lymphocytes and few plasma cells	Mostly macrophages and plasma cells with very few lymphocytes
Granuloma	Absent	Absent

Fig. 3. a. Representative IHC profiles of CD1a$^+$ dendritic cells from dermal biopsies of a healthy control, patient with polymorphic and macular PKDL (40X magnification).

b. Scatter plots showing the status of epidermal and dermal CD1a$^+$ dendritic cells in healthy controls (filled circle, n = 6), patients with polymorphic (filled square, n = 10) and macular (filled triangle, n = 10) PKDL; each horizontal bar represents the median value.

c. Representative IHC profiles of HLA-DR$^+$ cells from dermal biopsies of a healthy control, patient with polymorphic and macular PKDL (10X magnification)

d. Scatter plots showing the status of HLA-DR$^+$ cells in healthy controls (filled circle, n = 7), patients with polymorphic (filled square, n = 9) and macular (filled triangle, n = 8) PKDL. Each horizontal bar represents the median value.

415.60(183.80–903.50) pg/ml vs. 112.80(58.50–223.50) pg/ml, $p < 0.01$ and 39.23(31.43–58.78) pg/ml vs. 23.19(21.86–32.69) pg/ml, $p < 0.01$ respectively (Fig. 4c and d).

### 3.7. Increased CD8$^+$ T-cells only in polymorphic PKDL

Irrespective of the clinical variant, there was a preponderance of CD8$^+$ over CD4$^+$ T-cells in dermal lesions, with the CD4$^+$ subset being minimally present in almost all biopsies analysed (Fig. 5a and b). The proportion of CD8$^+$ T-cells increased by 16 fold in the polymorphic group as compared to healthy controls [31.9(21.85–38.95) vs. 2.0(0.75–6.05) cells mm^{-2}, $p < 0.01$]. However, in the macular form, CD8$^+$ T-cells were completely absent in some cases (n = 4) or comparable with healthy controls [1.8(0.6–2.75) vs. 2.0(0.75–6.05) cells mm^{-2}], (Fig. 5c and d). In polymorphic PKDL, the number of CD8$^+$ T-cells at the lesional site correlated positively with the parasite load (r = 0.61), but macular PKDL showed a negative correlation, r = −0.41.

3.8. Increase in CD20$^+$ B-cells greater in polymorphic PKDL

B-cells, as detected by CD20, increased in both variants as compared to healthy controls, being 6.5 fold higher in polymorphic cases [7.80(3.65–11.25) vs. 1.20 (0.80–1.80) cells mm^{-2}, $p < 0.05$] and 4 fold higher in the macular cases [4.80(2.20–7.00) cells mm^{-2}], Fig. 5e and f. Additionally, the circulating levels of CXCL13, the B-lymphocyte chemoattractant was elevated, being 18.28(14.26–22.88) vs. 11.68(9.88–13.92) pg/ml in healthy controls, $p < 0.01$ (Fig. 5g).

4. Discussion

PKDL since its identification by Brahmachari in 1922 has been clubbed as one entity with the polymorphic variant reigning supreme constituting > 90% of cases, while the remaining 10% were macular cases who present with innocuous hypopigmented lesions and importantly, do not actively seek treatment. It is only following implementation of the ongoing active surveillance programme that awareness of this neglected disease burden was enhanced (Sengupta
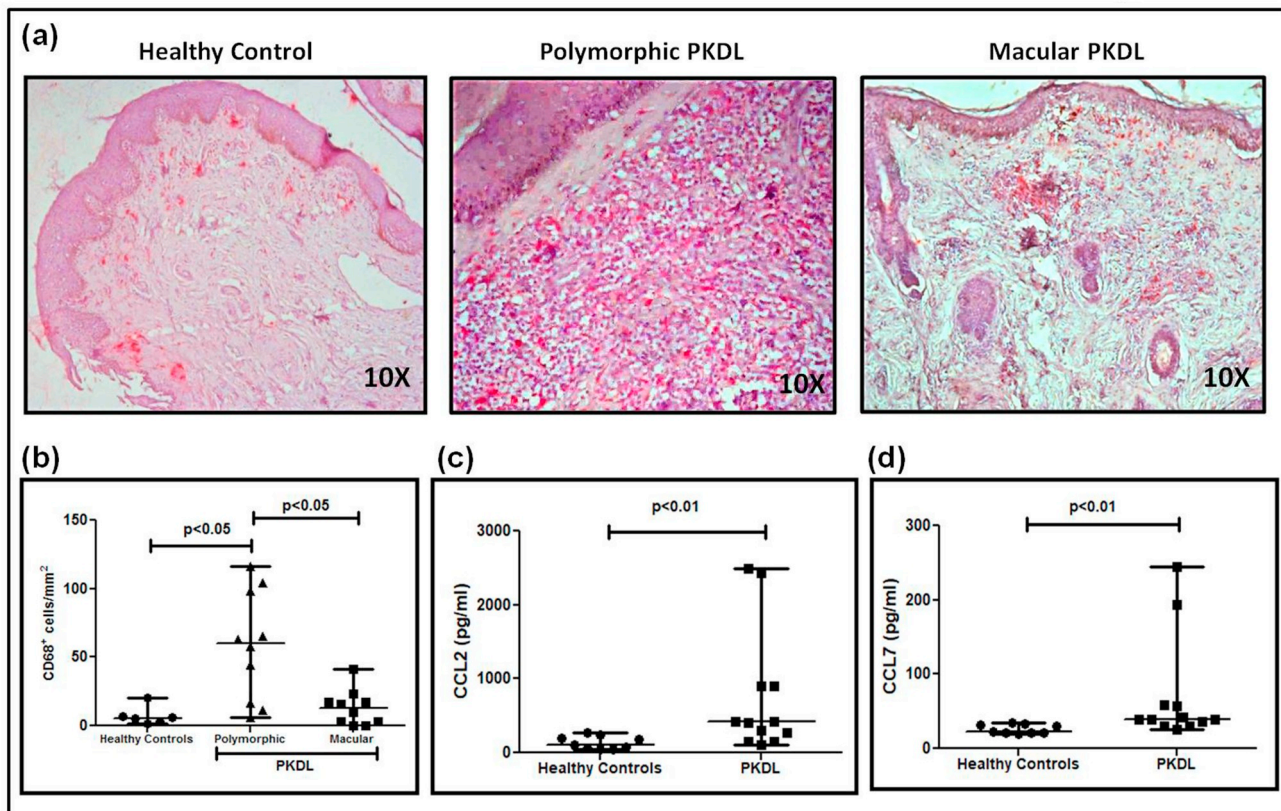
Fig. 4. a. Representative IHC profiles of CD68$^+$ cells from dermal biopsies of a healthy control, patient with polymorphic and macular PKDL (10X magnification). **b**. Scatter plots showing the status of CD68$^+$ cells in healthy controls (filled circle, n = 6), patients with polymorphic (filled triangle, n = 10) and macular (filled square, n = 10) PKDL. Each horizontal bar represents the median value.
c. Scatter plots indicating plasma levels of CCL2 in healthy controls (filled circle, n = 9) and patients with PKDL (filled square, n = 12). Each horizontal bar represents the median value.
d. Scatter plots indicating plasma levels of CCL7 in healthy controls (filled circle, n = 9) and patients with PKDL (filled square, n = 12). Each horizontal bar represents the median value.

et al., 2019). Furthermore, considering the overlapping features with other dermal variants of Leishmaniasis, it is important to distinguish the immunopathological characteristics of the two variants of Indian PKDL from that of CL or Sudanese PKDL. Accordingly, this study aimed to delineate the cellular milieu of the two variants, and provide more information on macular PKDL *vis-à-vis* its well defined polymorphic counterpart (Ganguly et al., 2010a; Zijlstra et al., 2003; Ramesh et al., 2015).

Irrespective of the geographical zone, dermal Leishmaniasis is distributed mainly in the face, neck, upper and lower extremities i.e. areas exposed to the bite of sandflies (Reithinger et al., 2007). However, in PKDL this does not hold true as lesions are more diffuse and in the polymorphic variant appear primarily on sun-exposed areas (Fig. 1a), similar to Sudanese PKDL, where the distribution of lesions often mirrors the clothing habits of those affected (Ismail et al., 2006a). This has been attributed to these areas having greater exposure to UV light (Ismail et al., 2006a) and suggested the possibility of Vitamin D polymorphism (Mukhopadhyay et al., 2014). However, with regard to the macular cases, this logic fails as their lesions are symmetrically distributed all over the body (Fig. 1b).

Studies on the overall histopathology of PKDL have established that akin to CL and African PKDL (Ismail et al., 2006b), there is a moderate to dense inflammatory cell infiltrate with lymphocytes being the predominant cellular component (Singh et al., 2015). However, this information is based on the polymorphic variant, as the infiltrate in macular cases was sparse and patchy comprising of lymphocytes, histiocytes and a few plasma cells (Fig. 2 a,b) in concordance with previous studies (Singh et al., 2015; Ramesh et al., 2008). This indicates

that despite the parasite being *L. donovani*, the two variants generate immunologically distinct immune responses, similar to tuberculoid and lepromatous variants of leprosy (Desvignes and Ernst, 2013). Furthermore, in view of the clinical features of polymorphic or macular PKDL overlapping with lepromatous or tuberculoid leprosy, as also its geographical overlap, it is important to differentiate to avoid unnecessary treatment. Unlike leprosy, where the infiltrate is patchy with a peri-appendageal location and a predilection for nerve bundles, in PKDL, the neural Schwann cells are usually unaffected with no loss of sensation. However, in terms of distribution, polymorphic PKDL was similar to CL and lepromatous leprosy, as the infiltrate encompassed the entire dermis (Ramesh et al., 2015; Gomes et al., 2017). However, in macular PKDL, the infiltrate remained confined to the upper section of the dermis (Fig. 2a and b). Furthermore, associated changes in the epidermis and dermis such as hyperkeratosis and focal papillomatosis were more frequently observed in the polymorphic variant (Fig. 2e, Table 2) whereas focal necrosis, a consistent feature in CL, was absent in both variants of PKDL.

The formation of granulomas results from an inflammatory interplay between a persistent, non-degradable antigen and the host's immune response, and translates into the release of pro-inflammatory cytokines as also chemokines along with activation of dendritic cells that transports the microbial antigen(s) to the lymph nodes (Aoun et al., 2014). This is followed by migration of activated T-cells to the granuloma, culminating in enhancement of the microbicidal activity of macrophages and limiting of the disease (Davis and Ramakrishnan, 2008). Classical examples are self-healing L-CL (Tuon et al., 2010; Gomes et al., 2017) and the African PKDL (Ismail et al., 2006b), but was
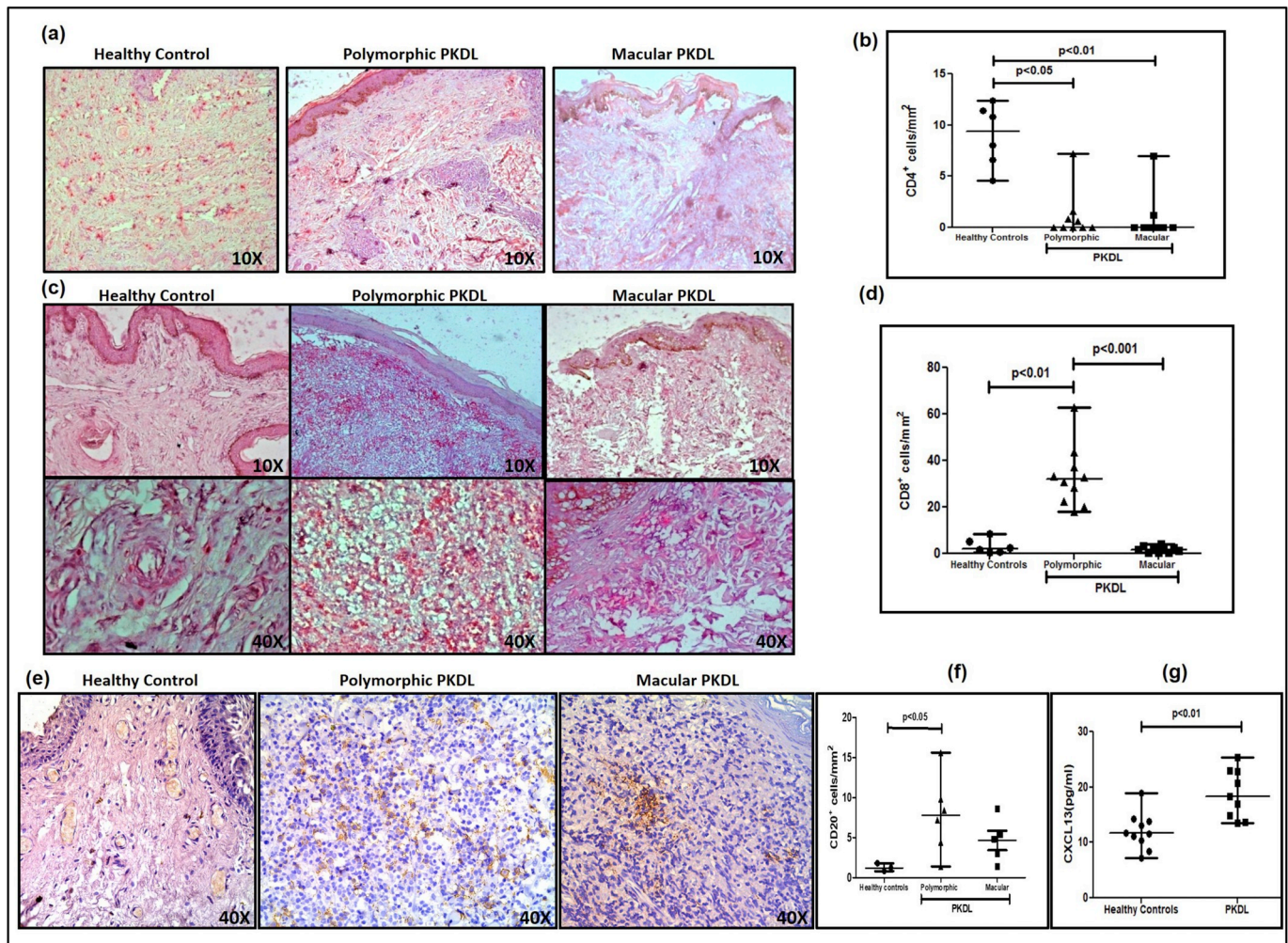
Fig. 5. a. Representative IHC profiles of CD4$^+$ T-cells from dermal biopsies of a healthy control, patient with polymorphic and macular PKDL (10X magnification). **b.** Scatter plots showing the status of CD4$^+$ T-cells in healthy controls (filled circle, n = 6), patients with polymorphic (filled triangle, n = 10) and macular (filled square, n = 10) PKDL. Each horizontal bar represents the median value.

c. Representative IHC profiles of CD8$^+$ T-cells from dermal biopsies of a healthy control, patient with polymorphic and macular PKDL (10X and 40X magnification). **d.** Scatter plots showing the status of CD8$^+$ T-cells in healthy controls (filled circle, n = 6), patients with polymorphic (filled triangle, n = 10) and macular (filled square, n = 10) PKDL. Each horizontal bar represents the median value.

e. Representative IHC profiles of CD20$^+$ B-cells from dermal biopsies of a healthy control, patient with polymorphic and macular PKDL (40X magnification).

f. Scatter plots showing the status of CD20$^+$ B-cells in healthy controls (filled circle, n = 3), patients with polymorphic (filled triangle, n = 6) and macular (filled square, n = 5) PKDL. Each horizontal bar represents the median value.

g. Scatter plots showing plasma levels of CXCL13 in healthy controls (filled circle, n = 10) and patients with PKDL (filled square, n = 9). Each horizontal bar represents the median value.

notably absent in Indian PKDL. IL-10 is known to inhibit granuloma formation as endorsed in a model of tuberculosis (Cyktor et al., 2013) and similarly, in lepromatous leprosy, IL-10 induced by type I interferons (IFN α/β) limits formation of granulomas (Teles et al., 2013). This possibly holds true for Indian PKDL as both variants demonstrated raised levels of IL-10 (Mukherjee et al., 2019; Ganguly et al., 2008).

Detection of LD bodies in slit skin smears or tissue biopsies is the gold standard and has been augmented by quantification of parasite load by qPCR (Moulik et al., 2018). In CL and African PKDL there was no correlation between the number of amastigotes and areas of inflammation and necrosis (Saldanha et al., 2017; Ismail et al., 2006b) whereas in the Indian variant, the dense, diffuse cell infiltrate in polymorphic PKDL correlated positively with parasite load (Fig. 2 c,d) and the presence of LD bodies. However, in all biopsies from macular cases, LD bodies were minimally present, even in cases where the parasite burden was comparable with polymorphic PKDL (Fig. 1c and d). This is in agreement with previous studies (Singh et al., 2015; Rathi et al., 2005), and suggests that perhaps the parasites are migrating

deeper into the dermis, reasons for which remain unanswered.

The skin, as a vital immune surveillance organ, continuously interacts with various infectious agents and generates an immune response dependent on the local inflammatory infiltrate (Morgado et al., 2018), with key contributors being dendritic cells via efficient induction of T-cell activation (Guermonprez et al., 2002). In patients with CL caused by *L. braziliensis,* the density of Langerhans cells (LCs) could be linked with disease severity (Feijó et al., 2016). Conversely, in Indian PKDL, a decreased presence of LCs was reported in the polymorphic variant (Mukherjee et al., 2015) and was mirrored to a lesser extent in macular cases (Fig. 3a and b). This was similar to Sudanese PKDL, where a similar scenario has been reported in terms of the dendritic cell number and morphology (Ismail et al., 2006a). As UVB rays can directly damage epidermal E-LCs (Clydesdale et al., 2001), it could account for their decrease being more pronounced in polymorphic lesions that appear mainly in sun exposed areas (Fig. 1a).

Leishmania-macrophage interactions are multifaceted and are dependent on the cytokine milieu and species (de Menezes et al., 2016), as

for example, in L-CL, the enhanced presence of Th1-associated cytokines leads to macrophages acquiring a heightened effector function and demonstrate a classically activated phenotype, as evidenced by CD68^{+} macrophages with an elevated iNOS (Saldanha et al., 2017, Nylén and Eidsmo, 2012). Conversely, in the more severe and chronic DCL, a Th2 milieu is present, along with alternative activation of macrophages with elevation of the arginase pathway that impedes protective immunity and promotes parasite growth (França-Costa et al., 2015). Similarly, in PKDL, the polymorphic variant demonstrated an increased presence of alternatively activated macrophages (Mukherjee et al., 2015; Mukhopadhyay et al., 2015), which correlated positively with parasite load and supported disease chronicity (Fig. 4 a,b). However, in macular PKDL, the proportion of CD68^{+} macrophages was substantially lower than the polymorphic variant (Fig. 4b), and in fact, correlated negatively with parasite load; their activation status remains to be delineated. Therefore, it may be proposed that in macular PKDL, the lower proportion of monocytes/macrophages accounts for their lower parasite load and translates into a milder disease profile. In view of the lower degree of infiltration of monocytes/macrophages at the lesional site in macular PKDL, it may have an impact on the lesional concentration of Liposomal Amphotericin B, as validated in a murine model of CL (Wijnant et al., 2018). Therefore, it is important that clinical trials be undertaken with a cohort representing both types of PKDL.

Antigen presenting cells use HLA-DR (MHC-II) molecules to present processed antigen to T-cells and in self healing CL, HLA-DR positivity was demonstrated in keratinocytes and granulomas (Pirmez et al., 1990). Similarly, in African PKDL, most cells in the dermis are HLA-DR[+] (Ismail et al., 2006b), possibly facilitating its self resolution. However in the Indian counterpart, the proportion of HLA-DR positivity was substantially decreased in both variants (Fig. 3c and d), the decrease being more prominent in the macular cases, possibly due to the lower infiltration of CD68^{+} macrophages (Fig. 4a and b) and CD1a^{+} dendritic cells (Fig. 3a and b).

The nature of T-cell responses often mirrors the disease outcome, and depending on their functional responses can be protective or deletorius (Novais and Scott, 2015). In Old World CL caused by *L. major*, CD4^{+} T-cells dominate the lymphocyte infiltrate (Nylén and Eidsmo, 2012; Geiger et al., 2010), whereas in the more severe forms of New World CL caused by *L. braziliensis*, cytotoxic CD8^{+} T-cells predominate (Novais et al., 2017). This CD8 T-cell cytotoxicity further activates the NLRP3 mediated inflammasome cascade leading to IL-1β release, accounting for the chronic inflammation (Novais et al., 2017). In Indian PKDL, there was an increased CD3 positivity (Ganguly et al., 2010b), but a consistent absence of CD4^{+} T-cells was noted (Fig. 5a and b). This was in contrast to the self-healing Sudanese PKDL, where CD4^{+} T-cells predominate (Ismail et al., 2006b), and it can therefore be proposed that this absence of CD4^{+} T-cells accounts for their inability to self heal. Furthermore, the study by Ganguly et al. (2010b) was mainly on the polymorphic variant and included only one macular case. In this study, differences emerged between the two variants regarding their proportion of CD8^{+} T-cells which were in abundance only in polymorphic lesions (Fig. 5c and d) and possibly account for their exaggerated inflammatory response. Conversely, the reduced presence of T-cells in macular PKDL possibly accounts for their relatively milder, cell mediated immune response (Fig. 5c and d).

In terms of the humoral immune response, B cells and plasma cells are present in lesional tissue, the proportion being higher in ulcerating CL (L-CL) than non-ulcerating chronic lesions of DCL (Vieira et al., 2002). These CD20^{+} cells are found usually in the middle of the dermis and do not differ between early and late lesions of CL (Saldanha et al., 2017). However, in African PKDL, B-cells are far fewer in number and in a minority of patients. In the Indian counterpart, the proportion of circulating CD19^{+} B-cells are decreased (Mukhopadhyay et al., 2012) whereas, in dermal lesions of both variants, an increased expression of CD20^{+} B-cells was demonstrated (Fig. 5 e,f). These B-cells possibly

support parasite persistence via facilitation of antibody mediated opsonisation of parasites into macrophages, as evident in experimental leishmaniasis (Kane and Mosser, 2001).

Infection with *Leishmania* induces chemokines to promote recruitment of leukocytes to lesional sites (Oghumu et al., 2010) and was corroborated in PKDL wherein increased levels of skin homing CCL17 and CCL22 was associated with an increased presence of CD8^{+} T-cells at the lesional sites (Mukherjee et al., 2019). In CL, CCL2 (Monocyte Chemoattractant Protein −1 or MCP-1) has been shown to play an important role in mediating recruitment of macrophages, monocytes, NK cells and other CCR2 expressing leukocytes (Allavena et al., 1994; Ritter and Moll, 2000), while CCL7 has been reported to attract Th2 cells to the lesional sites during infection with *L. major* (Katzman and Fowell, 2008). In PKDL, the consistent absence of Ki67 expression in dermal lesions in both variants confirmed dermal homing (Fig. 2f) and was corroborated by raised levels of CCL2, CCL7 and CXCL13, that accounted for the increased recruitment of macrophages and B-cells (Fig. 4c and d, 5g).

The scientific advances in our knowledge of the immune response in Leishmaniasis have allowed for excellent immunochemotherapeutic options to be developed and validated in animal models. However, the absence of an animal model for PKDL, as also limited availability of patients has led to its treatment remaining empirical and poorly defined (Pijpers et al., 2019). The natural history of PKDL suggests that it is not a static but a dynamic condition in which the parasite load, onset and appearance of the clinical presentation, as also tendency to self-heal vary with the developing immune response. What has been proven beyond doubt is that the immunological features of PKDL differ from VL, the systemic 'forerunner', in several aspects. It has been proposed that PKDL originates as an immune reconstitution inflammatory syndrome, resulting from a loss of immune suppression following drug treatment for VL (Amerson and Maurer, 2011). If VL is to be eliminated in South Asia, PKDL patients must be treated effectively and requires availability of robust data regarding the immunopathology of dermal lesions. As the development of PKDL is in all likelihood a host driven phenomenon, immune manipulation can be considered at several time points, (a) preventing the development of VL to PKDL (b) using immunomodulators like Miltefosine and (c) use of vaccines alone or combined with immuno-chemotherapy that may well have a therapeutic and/or prophylactic role (Osman et al., 2017). This study has delineated important differences between the polymorphic and macular variant, and could serve as a resource to underpin future mechanistic studies for guiding clinical research with a view towards achieving the critical goal of elimination of Leishmaniasis.

Declarations of interest

None.

Acknowledgements

References

Aara, N., Khandelwal, K., Bumb, R.A., Mehta, R.D., Ghiya, B.C., Jakhar, R., Dodd, C., Salotra, P., Satoskar, A.R., 2013. Clinico-epidemiologic study of cutaneous leishmaniasis in Bikaner, Rajasthan, India. Am. J. Trop. Med. Hyg. 89, 111–115.

Allavena, P., Bianchi, G., Zhou, D., van Damme, J., Jílek, P., Sozzani, S., Mantovani, A., 1994. Induction of natural killer cell migration by monocyte chemotactic protein-1, -2 and -3. Eur. J. Immunol. 24, 3233–3236.

Amerson, E.H., Maurer, T.A., 2011. Immune reconstitution inflammatory syndrome and tropical dermatoses. Dermatol. Clin. 29, 39–43.

Aoun, J., Habib, R., Charaffeddine, K., Taraif, S., Loya, A., Khalifeh, I., 2014. Caseating granulomas in cutaneous leishmaniasis. PLoS Neglected Trop. Dis. 8, e3255.

Arango Duque, G., Descoteaux, A., 2015. *Leishmania* survival in the macrophage: where the ends justify the means. Curr. Opin. Microbiol. 26, 32–40.

Burza, S., Croft, S.L., Boelaert, M., 2018. Leishmaniasis. Lancet 392, 951–970.

Clydesdale, G.J., Dandie, G.W., Muller, H.K., 2001. Ultraviolet light induced injury: immunological and inflammatory effects. Immunol. Cell Biol. 79, 547–568.

Cyktor, J.C., Carruthers, B., Kominsky, R.A., Beamer, G.L., Stromberg, P., Turner, J., 2013. IL-10 inhibits mature fibrotic granuloma formation during *Mycobacterium tuberculosis* infection. J. Immunol. 190, 2778–2790.

Das, N.K., Singh, S.K., Ghosh, S., Sarkar, A., Mukhopadhyay, D., Roy, S., Ganguly, D.N., Barbhuiya, J.N., Saha, B., Chatterjee, M., 2011. Case series of misdiagnosis with rK39 strip test in Indian leishmaniasis. Am. J. Trop. Med. Hyg. 84, 688–691.

Davis, J.M., Ramakrishnan, L., 2008. "The very pulse of the machine": the tuberculous granuloma in motion. Immunity 28, 146–148.

de Menezes, J.P., Saraiva, E.M., da Rocha-Azevedo, B., 2016. The site of the bite: *Leishmania* interaction with macrophages, neutrophils and the extracellular matrix in the dermis. Parasites Vectors 9, 264.

Desvignes, L.P., Ernst, J.D., 2013. Taking sides: interferons in leprosy. Cell Host Microbe 13, 377–378.

Feijó, D., Tibúrcio, R., Ampuero, M., Brodskyn, C., Tavares, N., 2016. Dendritic cells and *Leishmania* infection: adding layers of complexity to a complex disease. J Immunol Res 2016, 3967436.

França-Costa, J., Van Weyenbergh, J., Boaventura, V.S., Luz, N.F., Malta-Santos, H., Oliveira, M.C., Santos de Campos, D.C., Saldanha, A.C., dos-Santos, W.L., Bozza, P.T., Barral-Netto, M., Barral, A., Costa, J.M., Borges, V.M., 2015. Arginase I, polyamine, and prostaglandin E2 pathways suppress the inflammatory response and contribute to diffuse cutaneous leishmaniasis. J. Infect. Dis. 211, 426–435.

Ganguly, S., Das, N.K., Panja, M., Pal, S., Modak, D., Rahaman, M., Mallik, S., Guha, S.K., Pramanik, N., Goswami, R., Barbhuiya, J.N., Saha, B., Chatterjee, M., 2008. Increased levels of interleukin-10 and IgG3 are hallmarks of Indian post-kala-azar dermal leishmaniasis. J. Infect. Dis. 197, 1762–1771.

Ganguly, S., Das, N.K., Barbhuiya, J.N., Chatterjee, M., 2010a. Post-kala-azar dermal leishmaniasis-an overview. Int. J. Dermatol. 49, 921–931.

Ganguly, S., Mukhopadhyay, D., Das, N.K., Chaduvula, M., Sadhu, S., Chatterjee, U., Rahman, M., Goswami, R.,P., Guha, S.K., Modak, D., Mallik, S., Gonju, D., Pramanik, N., Barbhuiya, J.N., Saha, B., Chatterjee, M., 2010b. Enhanced lesional Foxp3 expression and peripheral anergic lymphocytes indicate a role for regulatory T cells in Indian post-kala-azar dermal leishmaniasis. J. Investig. Dermatol. 130, 1013–1022.

Geiger, B., Wenzel, J., Hantschke, M., Haase, I., Ständer, S., von Stebut, E., 2010. Resolving lesions in human cutaneous leishmaniasis predominantly harbour chemokine receptor CXCR3-positive T helper 1/T cytotoxic type 1 cells. Br. J. Dermatol. 162, 870–874.

Gomes, A.H.S., Martines, R.B., Kanamura, C.T., Barbo, M.L.P., Iglezias, S.D., Lauletta Lindoso, J.A., Pereira-Chioccola, V.L., 2017. American cutaneous leishmaniasis: in situ immune response of patients with recent and late lesions. Parasite Immunol. 39. https://doi.org/10.1111/pim.12423.

Guermonprez, P., Valladeau, J., Zitvogel, L., Théry, C., Amigorena, S., 2002. Antigen presentation and T cell stimulation by dendritic cells. Annu. Rev. Immunol. 20, 621–667.

Ismail, A., Khalil, E.A., Musa, A.M., El Hassan, I.M., Ibrahim, M.E., Theander, T.G., El Hassan, A.M., 2006a. The pathogenesis of post kala-azar dermal leishmaniasis from the field to the molecule: does ultraviolet light (UVB) radiation play a role? Med. Hypotheses 66, 993–999.

Ismail, A., Gadir, A.F., Theander, T.G., Kharazmi, A., El Hassan, A.M., 2006b. Pathology of post-kala-azar dermal leishmaniasis: a light microscopical, immunohistochemical, and ultrastructural study of skin lesions and draining lymph nodes. J. Cutan. Pathol. 33, 778–787.

Kane, M.M., Mosser, D.M., 2001. The role of IL-10 in promoting disease progression in leishmaniasis. J. Immunol. 166, 1141–1147.

Karunaweera, N.D., Pratlong, F., Siriwardane, H.V., Ihalamulla, R.L., Dedet, J.P., 2003. Sri Lankan cutaneous leishmaniasis is caused by *Leishmania donovani* zymodeme Mon-37. Trans. R. Soc. Trop. Med. Hyg. 97, 380–381.

Katzman, S.D., Fowell, D.J., 2008. Pathogen-imposed skewing of mouse chemokine and cytokine expression at the infected tissue site. J. Clin. Investig. 118, 801–811.

Kaushal, H., Bras-Gonçalves, R., Avishek, K., Kumar Deep, D., Petitdidier, E., Lemesre, J.L., Papierok, G., Kumar, S., Ramesh, V., Salotra, P., 2016. Evaluation of cellular immunological responses in mono- and polymorphic clinical forms of post-kala-azar dermal leishmaniasis in India. Clin. Exp. Immunol. 185, 50–60.

Masmoudi, A., Hariz, W., Marrekchi, S., Amouri, M., Turki, H., 2013. Old World cutaneous leishmaniasis: diagnosis and treatment. J Dermatol Case Rep 7, 31–41.

Molina, R., Ghosh, D., Carrillo, E., Monnerat, S., Bern, C., Mondal, D., Alvar, J., 2017. Infectivity of Post-Kala-azar Dermal Leishmaniasis patients to sand flies: revisiting a proof of concept in the context of the Kala-azar elimination program in the Indian subcontinent. Clin. Infect. Dis. 65, 150–153.

Mondal, D., Bern, C., Ghosh, D., Rashid, M., Molina, R., Chowdhury, R., Nath, R., Ghosh, P., Chapman, L., Alim, A., Bilbe, G., Alvar, J., 2018. Quantifying the infectiousness of post-kala-azar dermal leishmaniasis towards sandflies. Clin. Infect. Dis. https://doi.org/10.1093/cid/ciy891.

Morgado, F.N., de Carvalho, L.M.V., Leite-Silva, J., Seba, A.J., Pimentel, M.I.F., Fagundes, A., Madeira, M.F., Lyra, M.R., Oliveira, M.M., Schubach, A.O., Conceição-Silva, F., 2018. Unbalanced inflammatory reaction could increase tissue destruction and worsen skin infectious diseases - a comparative study of leishmaniasis and sporotrichosis. Sci. Rep. 8, 2898.

Moulik, S., Chaudhuri, S.J., Sardar, B., Ghosh, M., Saha, B., Das, N.K., Chatterjee, M., 2018. Monitoring of parasite kinetics in Indian post-kala-azar dermal leishmaniasis. Clin. Infect. Dis. 66, 404–410.

Mukherjee, S., Mukhopadhyay, D., Braun, C., Barbhuiya, J.N., Das, N.K., Chatterjee, U., von Stebut, E., Chatterjee, M., 2015. Decreased presence of Langerhans cells is a critical determinant for Indian Post kala-azar dermal leishman.iasis. Exp. Dermatol. 24, 232–234.

Mukherjee, S., Sengupta, R., Mukhopadhyay, D., Braun, C., Mitra, S., Roy, S., Kanti Das, N., Chatterjee, U., von Stebut-Borschitz, E., Chatterjee, M., 2019. Impaired activation of lesional CD8$^+$ T-cells is associated with enhanced expression of programmed death-1 in Indian post kala-azar dermal leishmaniasis. Sci. Rep. 9, 762.

Mukhopadhyay, D., Das, N.,K., De Sarkar, S., Manna, A., Ganguly, D.N., Barbhuiya, J.N., Maitra, A.K., Hazra, A., Chatterjee, M., 2012. Evaluation of serological markers to monitor the disease status of Indian post kala-azar dermal leishmaniasis. Trans. R. Soc. Trop. Med. Hyg. 106, 668–676.

Mukhopadhyay, D., Dalton, J.E., Kaye, P.M., Chatterjee, M., 2014. Post kala-azar dermal leishmaniasis: an unresolved mystery. Trends Parasitol. 30, 65–74.

Mukhopadhyay, D., Mukherjee, S., Roy, S., Dalton, J.E., Kundu, S., Sarkar, A., Das, N.K., Kaye, P.M., Chatterjee, M., 2015. M2 polarization of monocytes-macrophages is a hallmark of Indian post kala-azar dermal leishmaniasis. PLoS Neglected Trop. Dis. 9, e0004145.

Novais, F.O., Scott, P., 2015. CD8 + T cells in cutaneous leishmaniasis: the good, the bad, and the ugly. Semin. Immunopathol. 37, 251–259.

Novais, F.O., Carvalho, A.M., Clark, M.L., Carvalho, L.P., Beiting, D.P., Brodsky, I.E., Carvalho, E.M., Scott, P., 2017. CD8+ T cell cytotoxicity mediates pathology in the skin by inflammasome activation and IL-1β production. PLoS Pathog. 13, e1006196.

Nylén, S., Eidsmo, L., 2012. Tissue damage and immunity in cutaneous leishmaniasis. Parasite Immunol. 34, 551–561.

Oghumu, S., Lezama-Dávila, C.M., Isaac-Márquez, A.P., Satoskar, A.R., 2010. Role of chemokines in regulation of immunity against leishmaniasis. Exp. Parasitol. 126, 389–396.

Osman, M., Mistry, A., Keding, A., Gabe, R., Cook, E., Forrester, S., Wiggins, R., Di Marco, S., Colloca, S., Siani, L., Cortese, R., Smith, D.F., Aebischer, T., Kaye, P.M., Lacey, C.J., 2017. A third generation vaccine for human visceral leishmaniasis and post kala azar dermal leishmaniasis: first-in-human trial of Chad63-KH. PLoS Neglected Trop. Dis. 11, e0005527.

Pijpers, J., den Boer, M.L., Essink, D.R., Ritmeijer, K., 2019. The safety and efficacy of miltefosine in the long-term treatment of post-kala-azar dermal leishmaniasis in South Asia - a review and meta-analysis. PLoS Neglected Trop. Dis. 13, e0007173.

Pirmez, C., Oliveira-Neto, M.P., Grimaldi Júnior, G., Savino, W., 1990. Immunopathology of American cutaneous leishmaniasis. Modulation of MHC class II gene products by keratinocytes before and after glucantime therapy. Mem. Inst. Oswaldo Cruz 85, 203–209.

Ramesh, V., Ramam, M., Singh, R., Salotra, P., 2008. Hypopigmented post-kala-azar dermal leishmaniasis. Int. J. Dermatol. 47, 414–416.

Ramesh, V., Kaushal, H., Mishra, A.K., Singh, R., Salotra, P., 2015. Clinico-epidemiological analysis of Post kala-azar dermal leishmaniasis (PKDL) cases in India over last two decades: a hospital based retrospective study. BMC Public Health 15, 1092.

Rathi, S.K., Pandhi, R.K., Chopra, P., Khanna, N., 2005. Post-kala-azar dermal leishmaniasis: a histopathological study. Indian J. Dermatol. Venereol. Leprol. 71, 250–253.

Reithinger, R., Dujardin, J.C., Louzir, H., Pirmez, C., Alexander, B., Brooker, S., 2007. Cutaneous leishmaniasis. Lancet Infect. Dis. 7, 581–596.

Ritter, U., Moll, H., 2000. Monocyte chemotactic protein-1 stimulates the killing of *Leishmania major* by human monocytes, acts synergistically with IFN-gamma and is antagonized by IL-4. Eur. J. Immunol. 30, 3111–3120.

Saldanha, M.G., Queiroz, A., Machado, P.R.L., de Carvalho, L.P., Scott, P., de Carvalho, Filho, E.M., Arruda, S., 2017. Characterization of the histopathologic features in patients in the early and late phases of Cutaneous Leishmaniasis. Am. J. Trop. Med. Hyg. 96, 645–652.

Scholzen, T., Gerdes, J., 2000. The Ki-67 protein: from the known and the unknown. J. Cell. Physiol. 182, 311–322.

Sengupta, R., Chaudhuri, S.J., Moulik, S., Ghosh, M.K., Saha, B., Das, N.K., Chatterjee, M., 2019. Active surveillance identified a neglected burden of macular cases of Post Kala-azar Dermal Leishmaniasis in West Bengal. PLoS Neglected Trop. Dis. 13, e0007249.

Singh, A., Ramesh, V., Ramam, M., 2015. Histopathological characteristics of post kala-azar dermal leishmaniasis: a series of 88 patients. Indian J. Dermatol. Venereol. Leprol. 81, 29–34.

Teles, R.M., Graeber, T.G., Krutzik, S.R., Montoya, D., Schenk, M., Lee, D.J., Komisopoulou, E., Kelly-Scumpia, K., Chun, R., Iyer, S.S., Sarno, E.N., Rea, T.H., Hewison, M., Adams, J.S., Popper, S.J., Relman, D.A., Stenger, S., Bloom, B.R., Cheng, G., Modlin, R.L., 2013. Type I interferon suppresses type II interferon-triggered human anti-mycobacterial responses. Science 339, 1448–1453.

Tuon, F.F., Fernandes, E.R., Pagliari, C., Duarte, M.I., Amato, V.S., 2010. The expression of TLR9 in human cutaneous leishmaniasis is associated with granuloma. Parasite Immunol. 32, 769–772.

Vieira, M.G., Oliveira, F., Arruda, S., Bittencourt, A.L., Barbosa Jr., A.A., Barral-Netto, M., Barral, A., 2002. B-cell infiltration and frequency of cytokine producing cells differ

between localized and disseminated human cutaneous leishmaniases. Mem. Inst. Oswaldo Cruz 97, 979–983.

Wijnant, G.J., Van Bocxlaer, K., Fortes Francisco, A., Yardley, V., Harris, A., Alavijeh, M., Murdan, S., Croft, S.L., 2018. Local skin inflammation in Cutaneous Leishmaniasis as a source of variable pharmacokinetics and therapeutic efficacy of Liposomal Amphotericin B. Antimicrob. Agents Chemother. 24 e00631-18.

Zijlstra, E.E., Khalil, E.A., Kager, P.A., El-Hassan, A.M., 2000. Post-kala-azar dermal

leishmaniasis in the Sudan: clinical presentation and differential diagnosis. Br. J. Dermatol. 143, 136–143.

Zijlstra, E.E., Musa, A.M., Khalil, E.A., el-Hassan, I.M., el-Hassan, A.M., 2003. Post-kala-azar dermal leishmaniasis. Lancet Infect. Dis. 3, 87–98.

Zijlstra, E.E., Alves, F., Rijal, S., Arana, B., Alvar, J., 2017. Post-kala-azar dermal leishmaniasis in the Indian subcontinent: a threat to the South-East Asia Region Kala-azar elimination programme. PLoS Neglected Trop. Dis. 11, e0005877.